Sublimation of icy planetesimals and the delivery of water to the habitable zone around solar type stars

Adrián Brunini[1,2] María Cristina López[3]

1: CONICET
*2: Universidad Nacional de la Patagonia Austral. Ruta 3, acceso norte. Caleta Olivia, (9013). Santa Cruz, Argentina.*abrunini@yahoo.com.ar
3: Facultad de Ciencias Astronómicas y Geofísicas. Universidad Nacional de La Plata

Number of pages: 27
Number of Figures: 7
Number of Tables: 1

Proposed running head: **Delivery of water to the habitable zone.**

Correspondence should be directed to: Adrián Brunini. Universidad Nacional de la Patagonia Austral. Ruta 3, acceso norte. Caleta Olivia, (9013). Santa Cruz, Argentina.

Abstract

We present a semi analytic model to evaluate the delivery of water to the habitable zone around a solar type star carried by icy planetesimals born beyond the snow line. The model includes sublimation of ice, gas drag and scattering by an outer giant planet located near the snow line. The sublimation model is general and could be applicable to planetary synthesis models or N-Body simulations of the formation of planetary systems.

We perform a short series of simulations to asses the potential relevance of sublimation of volatiles in the process of delivery of water to the inner regions of a planetary system during early stages of its formation.

We could anticipate that erosion by sublimation would prevent the arrival of much water to the habitable zone of protoplanetary disks in the form of icy planetesimals. Close encounters with a massive planet orbiting near the outer edge of the snow line could make possible for planetesimals to reach the habitable zone somewhat less eroded. However, only large planetesimals could provide appreciable amounts of water. Massive disks and sharp gas surface density profiles favor icy planetesimals to reach inner regions of a protoplanetary disk.

Keywords: Planetary systems - Formation.

1 Introduction

The possible existence of habitable axoplanets is attracting a growing attention of the scientific community. There are more and more instruments dedicated to this task. Considerable effort has been devoted to developing semi analytic models and numerical simulations trying to predict the frequency of habitable planets in our Galaxy. One of the main ingredients for the rise of life on a planet is the existence of liquid water on its surface. Although different processes such as the presence of a planetary magnetic field, plate tectonics, and a planet massive enough to ensure the permanence of a stable atmosphere are decisive for the generation of life, so is the position of the planet with respect to the host star. The Habitable Zone (HZ) is defined as the circumstellar region within which a planet with similar characteristics to the Earth can permanently hold water in liquid state (Kasting et al. 1993, Kopparapu 2013; Selsis et al. 2007). The origin of water on planets harboring the habitable zone is a matter of debate. The firsts attempts trying to explain the origin of the Earthś water were based on the cometary delivery from beyond the giant planets region (Wetherill 1975; Chyba 1987; Ip & Fernández 1988; Delsemme 1992; Owen & Bar-Nun 2000). These studies were the base to models of the water delivery to terrestrial planets during terrestrial planet formation stages (Morbidelli et al. 2000; Chambers & Cassen 2002; Lunine et al 2003; Raymond, Quinn, & Lunine 2004; O'Brien, Morbidelli, & Levison 2006; Izidoro, Morbidelli, & Raymond 2014; Ciesla et al 2015; Dugaro et al. 2017). Alternatively, other models propose that water was delivered by planetesimals from Jupiter-Saturn region that were scattered onto high-eccentricity orbits by Jupiter, and thus crossing the terrestrial planet orbits (Walsh et al 2011; O'Brien et al 2014; Raymond & Izidoro 2017). At the same time, other models propose that icy pebbles may be the major contributors to the water on terrestrial planets (Sato, Okuzumi & Ida 2016).

Water-rich planetesimals come from beyond the distance to the central star known as the *snow line*, where the temperature is so low that water freezes. Once crossing inwards the snow line, water ice starts to sublimate.

Some accretion models included mass loss by sublimation, but only for the case of icy grains and small pebbles (Ciesla et al. 2015, Ida & Gillot 2016). In these models, grains and pebbles completely evaporates at the snow line, a situation which is not valid for larger objects such as km sized planetesimals. A fact well documented for comets in the solar system (Fernández 2005) is that the rate of sublimation is fast, but usually they spend thousands of years sublimating before complete disintegration.

For the case of solar system comets, the physical models of the dynamic

behavior of the volatiles were studied by Jorda, Crovisier & Green (1992) and applied by Tancredi, Rickman, & Greenberg (1994) and also by Tancredi (2006) to the Jupiter Family Comets. However, these models cannot be used directly to planetary accretion models, because they are developed for a particular case (the Sun is the central star, the comets have a particular kind of orbit and the snow line is fixed and located at a particular distance to the Sun). Sublimation models must be properly generalized to arbitrary planetesimal orbits and to the distribution of temperature in a generic protoplanetary disk, that in addition could vary during the disk evolution.

Although icy objects sublimates water from their surface when crossing inwards the snow line, accretion models including sublimation of icy planetesimals have not yet been developed. Therefore, the accretion of water by large planetesimals or planetary embryos forming in the HZ of a protoplanetary disk from planetesimals was not yet properly addressed.

One of the aims of this paper is to develop a simple model of the dynamical and physical behavior of icy planetesimals, appropriate to incorporate in planetary synthesis models (Ida, Lin & Nagasawa 2013, Miguel, Guilera & Brunini 2011), semi analytic models (Chambers 2016, Thommes, Duncan & Levison 2003, Brunini & Benvenuto 2008).

In addition, we will perform a small set of numerical simulations to asses if the sublimation of planetesimals would deserve to be included in further planetary accretion simulations.

In the next section we will describe the structure of the protoplanetary disk considered in our model and the physical effects included. Section 3 presents the results of our simulations and the last section is devoted to some conclusions.

2 The model

In this section we will present our basic disk model, and the different effects affecting the orbital and physical evolution of the planetesimals.

In all our simulations, planetesimals are perfectly spherical icy bodies, with bulk density $\rho_p = 1$ g cm^{-3}. Their initial radii r_p can be of 1, 10, or 100 km. Large planetesimals are included because recent models of planetesimal formation by gravitational instability tend to produce big planetesimals (Johansen et al 2015; Simon et al 2016, 2017; Schäfer, Yang, & Johansen et al 2017)

2.1 Central star and disk structure

We will adopt a $M_\star = 1M_\odot$ as the central star in all our simulations. For the disk model we will rely on the Minimum Mass Solar Nebula (MMSN) model of Hayashi (1981). The properties of the disk are summarized in the following set of equations. The gas surface density follow a power law of the form

$$\Sigma_g(R) = \Sigma_0\Big(\frac{R}{1AU}\Big)^{-\alpha}\mathrm{g/cm^2}, \tag{1}$$

where Σ_0 is the surface density at 1 AU. For the MMSN, $\Sigma_0 = 1700$ g cm^{-2}, $\alpha = 3/2$ (Hayashi 1981).

In this conditions

$$\rho_g(R) = 1.4\ f_g \times 10^{-9}\Big(\frac{R}{1AU}\Big)^{-(\alpha+5/4)}\mathrm{g\ \ cm^{-3}}. \tag{2}$$

Recent observations show that circumstellar disks around solar type stars have masses covering a wide range (Williams & Cieza 2011), spanning from ~ 0.1 to 10 MMSN. In our numerical simulations, following some previous works about planetary formation (Fortier, Benvenuto & Brunini 2007), we will adopt two different disk masses of 3 and 6 MMSN. The factor f_g in equation (2) is included for this purpose. Our standard disk model is the canonical MMSN given by Hayashi (1981), where the gas surface density index is $\alpha = 3/2$. Nevertheless, observations of circumstellar disks around young stellar objects support a wide range of power indexes with values of α in the range 0 – 1 (Williams & Cieza 2011). Therefore, we have also explored cases with $\alpha = 1$ and $\alpha = 1/2$. For each value of α, we have normalized the disk in such a way that the total mass inside 30 AU (a rather arbitrary outer limit, not affecting our results) is the same for disks with the same f_g.

One important parameter for our simulations is the lifetime of the disk. The inner disk fraction observed around stars in young stellar clusters and in the population of premain sequence stars in star-forming regions, point to a median disk lifetimes of between 2 and 3 Myr (Haisch, Lada, & Lada 2001; Hernández et al. 2008; Mamajek 2009; Fedele et al. 2010; Bell et al. 2013; Ribas et al. 2014; Richert et al. 2018) As it is usual in semianalytical models such as ours, we model the disk dispersal by an exponential decay

$$\rho_g(t) = \rho_g(0)e^{-t/\tau}, \tag{3}$$

where τ is the characteristic time scale of dissipation. In our case we will adopt $\tau = 3My$ for all our simulations.

The temperature profile in the disk is given by

$$T(R) = T(1AU)\Big(\frac{R}{1AU}\Big)^{-\beta}\mathrm{K}, \tag{4}$$

where $\beta = 1/2$ (Hayashi 1981). $T(1AU)$ is the temperature at $1AU$ for a given stellar mass, which in turn is related to the stellar luminosity through the Mass-Luminosity relation, and to the stellar radius. The Mass-Luminosoty relation is complex (see for example Eker et al. 2015). For stellar masses between 0.38 and 32 $M_\odot$ in the HR main sequence, the Mass-Luminosity relation is well fitted by single expressions of the form $L \propto M^\delta$. Eker et al. (2015) showed that this simple relation is preferable than other more complex expressions but the exponent δ changes at 1.05, 2, and 7 $M_\odot$. The effective temperature of main sequence stars can be obtained with an accuracy of $\sim$ 6%, as long their radii and mass can be obtained from observations with high accuracy (1% and 6% of relative error respectively). In the range of 0.5-3 $M_\odot$ a good single fit for the stellar effective temperature may be obtained from the calibration sample formed by main-sequence stars with accurate masses, radii and effective temperatures taken from Eker et al. (2014)

$$\frac{T_*}{T(1M_\odot)} = \psi\left(\frac{M_*}{M_\odot}\right)^{\kappa}, \tag{5}$$

where $\psi = 0.933 \pm 0.008$ and $\kappa = 0.62 \pm 0.016$. The temperature in the disk is important for the location of the *snow line* which is the distance to the central star where water ice starts to sublimate. Taking into account eq (5), the position of the snow line for a solar type star is given by

$$a_{ice} = a_{ice}(1M_\odot)\left(\frac{M_*}{M_\odot}\right)^{1.24}, \tag{6}$$

where $a_{ice}(1M_\odot)$ is the position of the snow line for a star of $1M_\odot$. The location of the snow line may evolve with time, and depends strongly on the dust size in the disk. For dust sizes like the ones of the interstellar medium (ISM), the snow line location range from 2 to 5 au for solar type stars, but for larger dust particles the snow line could be closer to the star (Oka, Nakamoto, & Ida 2011; Mulders et al. 2015), although in most theoretical models about the location of the snow line, grains of the size of ISM grains were considered, it is probable that larger grains were present in a protoplanetary disk. The position of the snow line also depends on the gas accretion rate onto the central star, which is far from being uniform for all solar type stars. In addition there is the question that a considerable amount of cosmochemical evidence in the solar system is arguing in favor of a fossilized snow line that

never was closer to the sun than 3 AU. A lot of work is still necessary to solve the inconsistency between the models of the evolution of the snow line location and the composition of the inner solar system (Oka, Nakamoto, & Ida 2011). Recent spectroscopic observations of protoplanetary disks (Blevins et al. 2016) show that the surface water abundance decreases by at least 5 orders of magnitude in the range of 3-11 AU for all the observed solar type stars. ALMA images also support this view (Banzatti et al. 2015). Therefore, given the complexity of the snow line location problem, we fix the snow line in our simulations. At present, the snow line in the solar system is located at $\sim$ 2.5 AU (Fernández 2005), where the temperature is around 182 K (Lodders 2003) and comets become active. For the simulations in this paper we adopt $a_{ice} = 2.7$ AU as the distance of the snow line for a $1M_{\odot}$ star, for the sake of consistency with the distance adopted in traditional semi analytic models of planet formation (Ida, Lin & Nagasawa 2013; Brunini & Benvenuto 2008, Chambers 2016). Our model, however, is general and a snow line moving with time could be incorporated for massive population synthesis simulations.

Another important concept we will use is the *Habitable Zone* (HZ) defined as the region where it would be possible for a planet to harbor life. The location of the HZ in a planetary system depends mainly on the distance to the central star and the stellar luminosity, but it also depends on the mass of the planet and the type of its atmosphere. A conservative inner limit is the distance from the central star where a runaway greenhouse effect vaporizes the water on the planet surface. The outer boundary is where the surface temperature of the planet is below the freezing point of water (Lammer et al. 2009, Kasting et al. 1993). For simplicity, we will use the definition given by Kopparapu et al. (2013) for a solar mass star

$$1AU \leq a_{HZ} \leq 1.7AU. \tag{7}$$

2.2 Gas drag

The nebular gas interacts with the planetesimals, causing damping of their orbital eccentricities and inclinations, and the decay of their orbits toward the central star. Eventually, they could reach the snow line and start to sublimate material and loss mass. Due to the pressure support in the nebula, the gas velocity is slower than keplerian by a small amount

$$\eta = \frac{v_k - v_g}{v_k} = \frac{16}{\pi}(\alpha + \beta)\Big(\frac{c_s}{v_k}\Big)^2, \tag{8}$$

where v_k and v_g are the keplerian and the gas velocity at a given distance to the central star respectively. c_s is the sound speed in the disk

$$c_s = \sqrt{kT/\mu_g}, \tag{9}$$

where k is the Boltzmann constant, and m_g is the the mean molecular weight of the gas disk (we adopt $\mu_g = 1.15\mu_{H_2}$, with μ_{H_2} the weight of the Hydrogen molecule). A typical value of η is of the order of 10^{-3}.

In addition, if the orbit of the planetesimal is not circular, the planetesimal have a mean relative velocity respect to the gas given by (Adachi, Hayashi & Nakazawa; 1976)

$$v_{rel} = v_k \sqrt{\eta^2 + \frac{5}{8}e^2 + \frac{1}{2}i^2}, \tag{10}$$

which is only valid for small e and i, the orbital eccentricity and inclination of the planetesimal.

Following Rafikov (2004), we consider several drag regimes, according to the size of the planetesimal r and the turbulence of the disk

- Epstein regime if $r < \lambda_{H_2}$,
- Stokes regime if $r > \lambda_{H_2}$ and $R_e < 20$,
- Quadratic regime if $r > \lambda_{H_2}$ and $R_e > 20$,

where λ_{H_2} is the mean free path of the molecular Hydrogen (Adachi 1976)

$$\lambda_{H_2} = \frac{\mu_{H_2}}{\sqrt{2}\rho_g d_{H_2}}, \tag{11}$$

where d_{H_2} is the size of the Hydrogen molecule.

The different drag regimes can be characterized by the stopping time, given by

$$t_{stop} = \begin{cases} \frac{\rho r}{\rho_g c_s} & \text{Epstein regime} \\ \frac{2\rho r^2}{3\rho_g c_s} & \text{Stokes regime} \\ \frac{6\rho r}{\rho_g v_{rel}} & \text{Quadratic regime,} \end{cases} \tag{12}$$

where ρ is the bulk density of the planetesimals.

In our simulations $t_{stop} >> P_{orb}$. In this condition, the secular change in the planetesimal orbit due to gas drag is given by

$$\begin{aligned} \frac{de^2}{dt} &= -\frac{2e^2}{t_{stop}}, \\ \frac{di^2}{dt} &= -\frac{2i^2}{t_{stop}}, \\ \frac{da}{dt} &= -\frac{2a\eta}{t_{stop}}. \end{aligned} \tag{13}$$

The previous expressions are not accurate for an orbit with high eccentricity. In this case, Kobayashi (2015) proposed some corrections to the secular variations computed with (13). These corrections are remarkably simple

$$\begin{aligned} \frac{de^2}{dt} &= \left(\frac{de^2}{dt}\right)_{low}(1-e^2)^{-\alpha+\beta-3/2}, \\ \frac{di^2}{dt} &= \left(\frac{di^2}{dt}\right)_{low}(1-e^2)^{-\alpha+\beta-1/2}, \\ \frac{da}{dt} &= \left(\frac{da}{dt}\right)_{low}(1-e^2)^{-\alpha+\beta-1/2}, \end{aligned} \tag{14}$$

where the quantities denoted with the sub index *low* are the ones computed with the set of equations (13). We implemented these expressions to compute the effect of gas drag on the planetesimals in all our numerical experiments.

2.3 The sublimation of ice

Once icy planetesimals enter into the warm regions of the disk, they may start to sublimate ice from their surface. It is well known that this process occurs in the comets of the solar system. In the context of planetary formation, some previous works considered the process of sublimation of small dust grains, but to our knowledge, no previous attempts to model sublimation of ices in planetary formation stages where large planetesimals and planetary embryos coexist were done.

The sublimation rate per unit surface of an icy object is usually assumed to be a function of its surface temperature only (Delsemme 1984), and may be written in the form

$$\frac{dm}{dt} = \frac{a_1}{\sqrt{T}} e^{-a_2/T}, \tag{15}$$

where T is here the temperature on the planetesimal surface, and a_1, a_2 are constants. The temperature of the planetesimal surface depends on the

balance between the input solar radiation, and the the losses of energy by thermal infrared radiation, sublimation of ices, and heat conduction into the planetesimal interior (Fernández 2005). This balance depends on several complex and not completely known factors such as the infrared albedo and thermal conductivity of the planetesimal. Moreover, the temperature of the surface could be not exactly the equilibrium black body temperature, since the sublimated ice carries away much of the heat as latent heat of sublimation. In addition, the solar radiation does not reach the surface because of the radiation extinction due to the possible formation of a coma around the planetesimal nucleus. All these factors difficult the building of an accurate model of the sublimation of ices on the planetesimal surface.

Based on estimations of the lifetimes of Short-Period Comets, Di Sisto, Fernández & Brunini (2010) have given an empirical expression for the sublimation rate in the region inside the snow line

$$\begin{aligned}\Delta m = 1074.99 - 4170.89q + 8296.96q^2 - 8791.78q^3 + \\ 4988.9q^4 - 1431.4q^5 + 162.975q^6,\end{aligned} \tag{16}$$

where q is the perihelion distance of the object in AU, Δm is the mass loss per orbital period and per unit surface of the object in $g\ cm^{-2}$. This expression is valid for Short Period Comets, whose orbits are dynamically dominated by Jupiter. In what concern to the sublimation rate, the most important fact is the time an object spends at a given distance $r < a_{ice}$ from the central star, because the temperature on the surface will be a function of it through equation (4). Most Jupiter Family Comets have orbits with aphelion distances near the semi major axis of Jupiter (70 per cent of the known Jupiter Family Comets have aphelia between $a_{Jupiter} \pm 0.5$ AU). However, we need a sublimation model valid for any orbit. In order to accomplish this task, we used the expression (15) to model the sublimation rate of ice, fitting the coefficients a_1 and a_2 to match the behavior of comets given by equation (16). We defined a population of objects, all with aphelion distance $Q = 5.2AU$ and different perihelion distances in the range $0.5 \leq q \leq 2.7$ AU. For each one of them, we have performed an integration of the sublimation rate along one orbital revolution as

$$\Delta m = \int_{t_0}^{t_1} \frac{a_1}{\sqrt{T}} e^{-a_2/T} dt, \tag{17}$$

where t_0 and t_1 are the times where the object enters and comes out from the region $r \leq 2.7AU$. a_1 and a_2 where left as free parameters to be determined in order to get the best fit to the values given by equation (16). The final values of the parameters are $a_1 = 0.12$ and $a_2 = 1865$ to get Δm in $g\ cm^{-2}$

per orbital revolution. We then used these set of coefficients together with equation (17) as the sublimation model in our simulations.

At each excursion inside the snow line, the radius of a perfectly spherical planetesimal is reduced by an amount

$$\frac{\Delta r}{r} = \frac{\Delta m}{3m}. \tag{18}$$

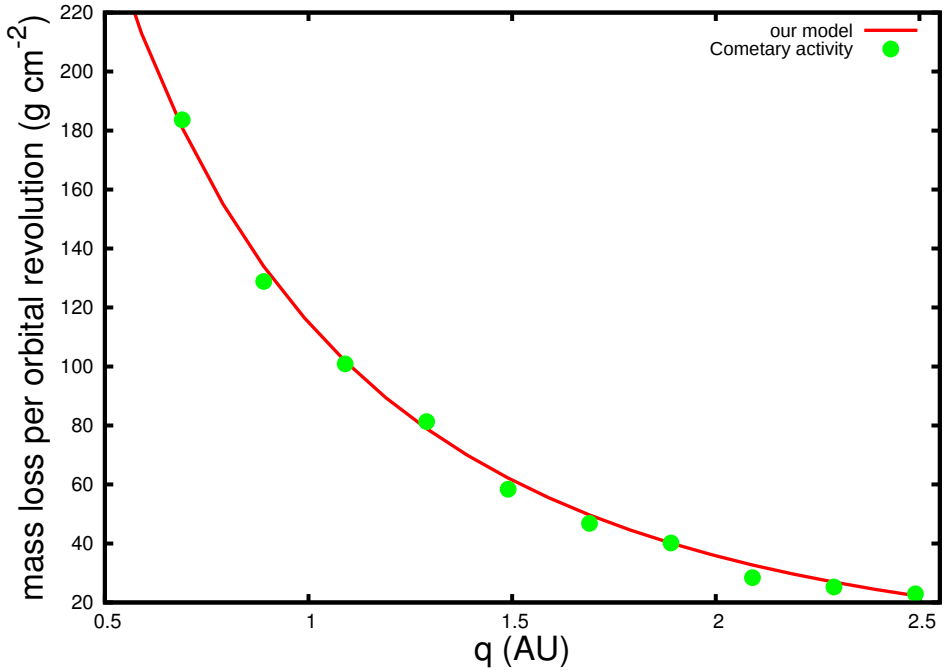

Figure 1: ***Sublimation rate of spherical icy objects per surface unit and per orbital revolution, as a function of the pericentric distance.***

The comparison between this approximation and the results given by equation (16) is shown in Figure 1 for our sample of objects. For icy objects, the volatile material is mixed with dust particles of different sizes. In the case of periodic comets, as a result of the sublimation of its ices once entering the inner planetary region, a dust mantle may develop. There is a maximum size from which the gas can no longer drag the dust particles from the comet surface. For a solar type star, this size is of the order of the cm at 1 AU (if the dust particles are smaller than this critical size, there is no chance to form a dust mantle). Larger particles stay on the surface (Rickman et al

1990). However, to consolidate a permanent crust, an increase of the perihelion distance is necessary, in order to stop the sublimation process (Kuehrt & Keller 1994, Möhlmann 1995). When a comet approaches the Sun in the next passage through the inner planetary region, the dust particles will be removed as the heat wave reaches the underlying ices, so the dust mantle may be partially or entirely removed (Fernández 2005). In fact, the buildup and complete remotion of a dust mantle may be cyclic, as the comet approaches and recedes from the Sun. If the dust mantle is consolidated and thick enough, the heat wave may increase the internal pressure in the comet, causing its fracture and further splitting. For a migrating planetesimal on a nearly circular orbit, the surface temperature always grows as it spiral towards the Sun. In this case it is difficult to anticipate if a permanent dust mantle could form, or if the sublimation could proceed up to the complete disintegration. In our model we considered that the sublimation process does not stop until the planetesimal is entirely disintegrated. We have also neglected splittings and other disruptive mechanisms that seem to be common in cometary behavior. Given the uncertainties in the sublimation model, the sublimation rate given by equation (15) was multiplied by a factor $f \leq 1$.

2.4 some preliminary results

In this section we will show the evolution of planetesimals evolving from outside the snow line. We run cases with 1 MMSN, and 6 MMSN with power index $\alpha = 1$, around a $1M_{\odot}$ star. The planetesimal radius is $r = 100$ km and f, the factor of sublimation, was set equal to 0.5. In Figure (2) we show the evolution of the planetesimal radius vs. the pericentric distance.

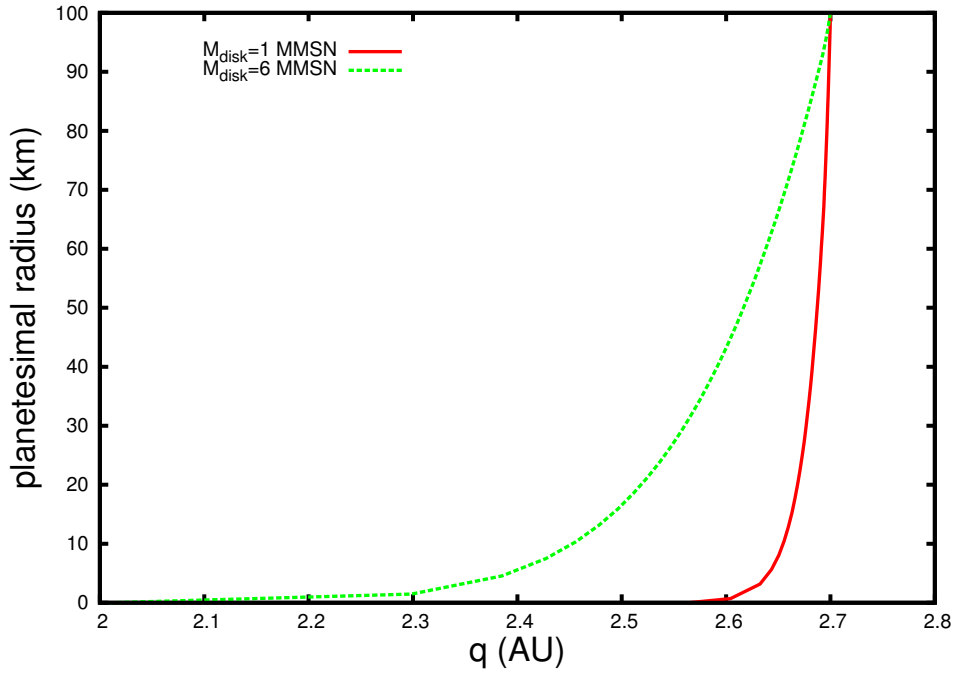

Figure 2: ***The fate of a 100 km planetesimal for two different nebular masses. The competition between orbital decay by gas drag and surface erosion by sublimation of ice makes the planetesimal to reach innermost regions of the disk for more massive nebulae.***

In both cases the planetesimal was launched on a circular orbit at 2.7 AU. A competition between the inwards migration by gas drag, and erosion by sublimation of ice becomes evident. The planetesimal reaches more internal regions of the disk when the nebula is more massive. In neither case is water deposited in the habitable zone. In this model, where planetesimals reach the snow line already on circular orbit, no much water is to be expected to reach the HZ.

2.5 Scattering by a protoplanet

When a planetesimal approaches a protoplanet at a small distance, its orbit changes due to the gravitational interaction between them. If the protoplanet is massive enough, the orbital change may be very strong. In the context of the problem we are investigating, it would be possible that the interaction with a planet that orbits near the snow line excites the orbit of the planetesimals, sending them directly inside the habitable zone without suffering too

much loss of mass by sublimation. This is the case of some models of water delivery to the primitive Earth, in which there is a population of planetesimals scattered by Jupiter/Saturn onto high-eccentricity orbits which cross the terrestrial planets (Walsh et al. 2011; O'Brien et al. 2014; Matsumura, Brasser, & Ida 2016; Raymond & Izidoro 2017). To address this possibility, we have to model this interaction, but in a very simple way, so as not to lose the speed of calculation allowing the code to be able to perform massive simulations for a planetary synteshis approach. N-Body numerical integration is not appropriate for this task.

In what follows we will consider the planet on circular orbit of radius a_p. We will also consider that the encounter takes place at a distance $r = a_p$ from the central star. At each orbital period of the planetesimal, we evaluate if an approach to the planet at a distance less than the Planet Hills distance R_H, defined as

$$R_H = a_p\Big(\frac{m_p}{3M_\star}\Big)^{(1/3)}, \tag{19}$$

would be possible (e.g. if the point of minimum distance between both orbits is less than this distance). If the answer is positive, we compute the probability that this close approach actually happens. The computation of the probability of a close encounter between two orbiting objects must be made taking into account different encounter geometries. If the orbits of the two objects intersects, we can use the classical formulation due to Öpik (1951) for the probability of encounters at a distance less than a given radius D. Per orbital period of the planetesimal it is given by

$$P_{enc} = \frac{4\pi a_p D U}{v \sin\theta}, \tag{20}$$

where v is the planetesimal velocity in units of the planet orbital velocity. U the relative velocity of the encounter in units of the planet orbital velocity and θ is the angle between the velocity vectors of the planet and the planetsimal during the closest approach. It results evident that this expression becomes singular for the case of tangential orbits, as the two velocity vectors becomes aligned. As θ approaches 0 there is a transition to the "*tangential regime*" where the probability of a close approach to a distance less than D must be computed in a different way (JeongAhn & Malhotra, 2017)

$$P_{enc} = \begin{cases} \frac{1}{T_P}\sqrt{\frac{8(1-v)D}{(1+v)g\sin\alpha}} & \text{Intersecting orbits} \\ \frac{1.7}{T_p}\sqrt{\frac{(1-v)D}{(1+v)g\sin\alpha}} & \text{Non intersecting orbits,} \end{cases} \tag{21}$$

where T_p is the orbital period of the planet and g is the gravitational accel-

eration due to the central star in the vicinity of the encounter. We have

$$\sin\alpha = \frac{a(1-e^2)}{a_p\sqrt{2(1-e^2)+e^2-1}}. \tag{22}$$

The transition from intersecting to non intersecting orbits occurs approximately at (JeongAhn & Malhotra, 2017)

$$\theta_c \simeq \sqrt{\frac{(1-v^2)Dg\sin\alpha}{v^2 v_p}}. \tag{23}$$

Once computed the probability P_{enc}, the mean time interval between close encounters is given by

$$\Delta T_{enc} = P_{enc}^{-1}. \tag{24}$$

The way to generate $N = T_{tot}/\Delta T_{enc}$ times of occurrence of close encounters during a time interval T_{tot}, is through the generation of random numbers $t_i;\ i = 1, 2...N$ with uniform distribution in the interval $[0, T_{tot}]$, and sorting them in an increasing sequence. In our case, the orbit of the planetesimal is changing at each orbital period, and therefore also changes T_{enc}. To compute the encounters, we repeat the random generation and sorting at each time step. If t_1, the smaller time in the sequence, is less than the orbital period of the planetesimal, which we adopted as the step size of the simulation, then we assume that a close encounter actually happens, and we proceed to its computation. This is done by means of a numerical integration of the star-planet-planetesimal Restricted Three Body Problem. We have checked that this procedure gives random times with uniform distribution and correct mean and r.m.s. for the case of not changing orbits. As initial conditions to start the numerical integration, the planetesimal is placed at random on the Hills sphere of the planet, and the relative velocity vector is directed to the interior of the Hills sphere following Henon's recipe (Henon, 1972). The relative velocity is given by

$$U = \sqrt{3 - T_{iss}}, \tag{25}$$

where T_{iss} is the Tisserand parameter, that may be written in terms of the perihelion distance q, the aphelion distance Q and the relative inclination of the planetesimal with respect to the orbital plane of the planet, as

$$T_{iss} = \frac{2}{q+Q} + 2\sqrt{2qQ/(q+Q)}\cos i. \tag{26}$$

In this expression, q and Q are measured in units of a_p. The integration is carried out with a Bullirsch-Stöer high precision routine. The routine and precision is the same than the one used in the N-Body integration package EVORB (Fernández, Gallardo, & Brunini 2002). During close encounters, the effect of gas drag was not included. For this preliminary investigation, the possible presence of an extended atmosphere of the planet is not considered.

3 Results

We have run simulations varying several parameters:

- The planetesimal radius (1 km, 10 km and 100 Km).
- The density of the nebula (3 and 6 MMSN).
- The power index α of the gas surface density ($\alpha = 3/2$, $\alpha = 1$ and $\alpha = 1/2$).
- The mass of the planet responsible for the scattering of planetesimals ($m_p = 1 M_{Jupiter}$, $100 M_\oplus$ and $10 M_\oplus$.
- The location of the planet ($a_p = 3$ AU and $a_p = 4$ AU).
- The factor of sublimation rate $f = 1$ and $f = 0.5$.

We have run 1000 planetesimal for each one of these set of parameters. In total we have analyzed the behavior of 15,000 initial conditions.
The end states reached in the simulations are:

1. The planetesimal evolves with $r > 100$ m up to the end of the simulation (The total time spam is $T_{tot} = 10^7$ y. 100 m is the size we consider for the planetesimal to be completely evaporated.
2. The planetesimal radius reduces by sublimation up to $r < 100m$. In this situation the simulation stops. We consider that the planetesimal evaporates completely.
3. During a close encounter, the planetesimal collides onto the giant planet.
4. After a close encounter, the planetesimal is ejected from the planetary system on hyperbolic orbit.

If the planetesimal radii becomes $r < 100$ m, we stop the simulation. Regarding the initial conditions for the planetesimal orbits we set them in order to guarantee starting on planet crossing orbits. The pericentric distance is set to $q = a_p - R_H$ and the apocentric distance to $Q = a_p + 3R_H$. These values were chosen in order to have planetesimals not too inside the inner region of the disk so to artificially favor the delivery of water to the habitable zone. We have made a huge quantity of preliminary runs. We found that for larger values of Q the fast circularization of the obit due to gas drag makes q to increase, and close encounters with the giant planet are quickly prevented. These cases are not of interest for our study. The orbital inclination of the planetesimals was set to $i = 5°$. If not explicitly stated, all the results correspond to simulations with $\alpha = 3/2$, $f = 1$ and $f_g = 6$.

This scenario is one of the assumed by most planetary synthesis formation codes (Ida & Lin 2004a, 2004b, 2005, 2008a, 2008b, 2010); Ida, Lin & Nagasawa 2013; Chambers 2008, 2013, 2014, 2016; Miguel & Brunini 2008, 2009, 2010). Giant planets form when the disk is already plenty of gas. If the core instability hypothesis (Mizuno, 1980) is the formation mechanism of giant planets, solid cores of several Earth masses form before the nebular gas dissipates. For most disk around solar type stars, the gas disk lifetime is of the order of few My, as adopted in our model. Therefore, when the gas is already present and abundant in the disk, 1-100 km planetesimals should exist (the cores of the giant planets form through accretion of planetesimals) together with one or several cores of giant planets, because they should form before the complete remotion of the gas. Therefore, we consider that our scenario is completely consistent with what is expected for the first 10 My of evolution of a planetary systems.

In the Figure (3) we show two typical evolution of a 100 km planetesimal with a 1 $M_{Jupiter}$ planet. In the upper panels we show the orbital evolution (left) and the radius of the planetesimal (right). During successive close encounters with the giant planet, the planetesimal enters into the HZ. The sublimation during the excursions inside the temperate regions of the disc reduces the diameter of the planetesimal in a few km. But a last close encounter pulls the apocentric distance to ~ 4.5 AU. The orbit circularizes at a given rate given by the corresponding stopping time. If it is longer than the mean time between collisions, the pericentric distance becomes larger than $a_p + R_H$. In this situation, close encounters are no longer possible, and the orbit of the planetesimal slowly becomes more and more circular. The semimajor axis decreases slowly by gas drag, but as the nebular gas dissipates, the planetesimal ends up in an outer orbit never being eroded by sublimation. In ~ 50 per cent of the cases where ejection from the system or a collision onto the planet do not occurs, the planetesimal evolution is like this one.

The evolution in the other half of the cases is as shown in the lower panels. Close encounters reduce the pericentric distance well below the planetary orbit, where circularization prevents further close encounters, in a mechanism similar to the one described for the previous case. The circularization proccedd faster than orbital decay by one order of magnitude. Orbital decay starts to be slow, but the size of the planetesimal is strongly reduced by sublimation, reinforcing the effect of gas drag. The semimajor axis decays and the planetesimal quickly evaporates completely. In this particular case, the planetesimal does not reach the HZ before its complete evaporation, although this is not what always happens.

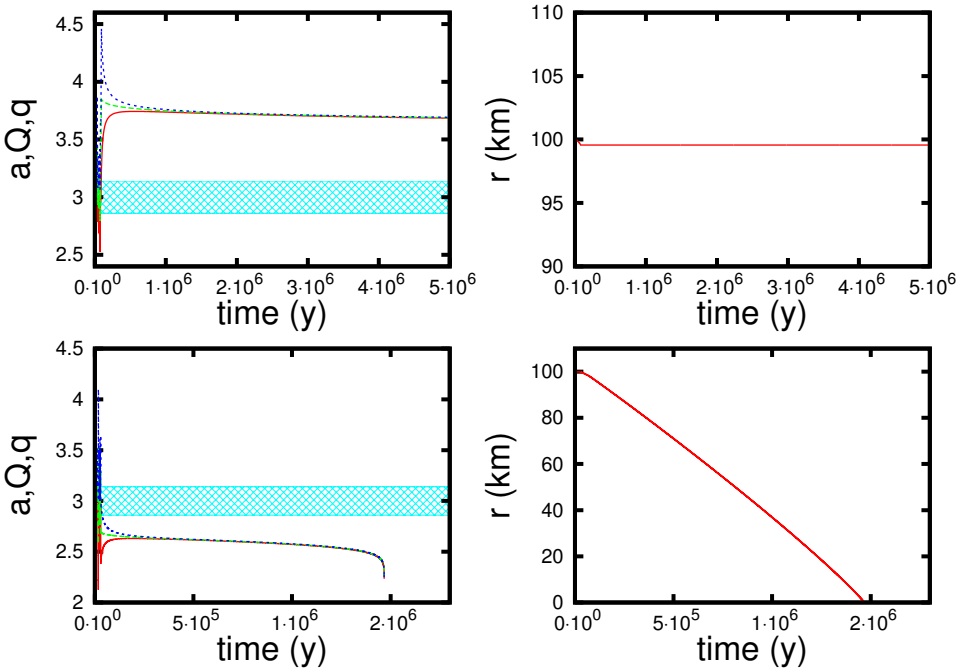

Figure 3: ***Typical orbital and physical evolution of a 100 km planetesimal. A fraction of them evolve outwards, ending up beyond the planetary orbit. An important fraction migrate inwards. Orbital circularization is fast, and the planetesimals migrates to regions were the sublimation of ice is effective. The shaded region is the corresponding to*** $a_p \pm R_H$.

As we are interested in the quantity of water that enters into the HZ from planetesimals formed outside the snow line, we will show our result as the cumulative distributions. To do this, at each time step we sum the total

mass that is in bins of 0.05 AU wide in the range 0 - 2.7 AU. In Figure 4 we show the effect produced by the the distance of the giant planet to the outer edge of the snow line. The result is not surprising. If the planet is at 4 AU, planetesimals enter into the sublimation region already with a rather circularized orbit due to gas drag, and the behavior is similar to the one shown in Figure 3.

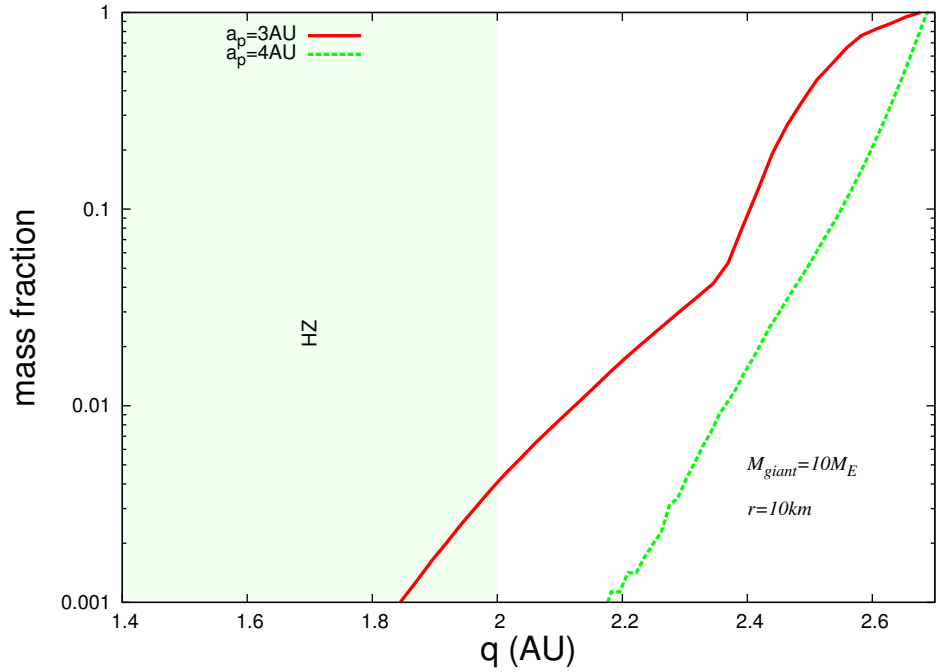

Figure 4: ***The fraction of water within the snow line delivered from beyond it for the cases of a*** $10M_{\oplus}$ ***planet at 3 and 4 AU.***

In the case of $a_p = 3$ AU, an accumulation of mass at $q > 2.3$ AU is observed. The minimum perihelion distance a planetesimal can reach after a close encounter with a planet is given by (Fernández 1984)

$$q_{min} = a_p(1-U)^2/(1+2U-U^2), \tag{27}$$

For our numerical experiments, considering $q = (a_p - R_H)/a_p$ and $Q = (a_p + 3R_H)/a_p$, the q_{min} obtained for different planetary masses and $a_p = 3$ AU are shown in Table 1.

In Figure 4 we can observe that the value of q is a bit smaller than the one reported in Table 1 but this is because the planetesimals arrive there after several close encounters and not just one.

M_p	q_{min} (AU)
10 $M_\oplus$	2.57
100 $M_\oplus$	2.18
1 $M_{Jupiter}$	1.90

Table 1: ***Minimum pericentric distance a planetesimal can reach after a close encounter.***

In Figure 5 we show the evolution of the planetesimals of different radii for planets of 10 $M_\oplus$, 100 $M_\oplus$ and 1 $M_{Jupiter}$.

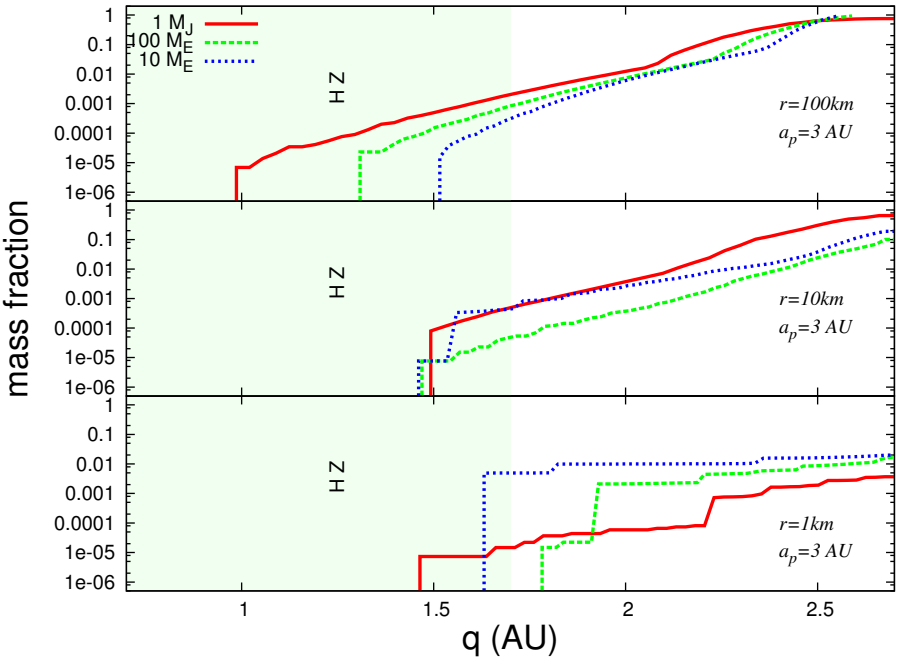

Figure 5: ***The fraction of water within the snow line delivered from beyond it for different planetary masses. In all the cases,*** $a_p = 3$ ***AU. The mass fraction is normalize to the case of*** $r = 100$ ***km.***

Only massive planets and/or large planetesimals, can guarantee some delivery of water into the HZ. In general, planetesimals of 1-10 km do not reach efficiently the HZ as to provide enough water to terrestrial planets in the HZ. For the case of $r = 100$ km and $r = 1$ km, equivalent quantity of mass cross the snow line, because in spite of being less massive, the smaller

planetesimals suffer a faster decay due to gas drag. However, sublimation of ice eroded them quickly. In the case of smaller planetesimals, the mass entering into the sublimation region is very small. To compute the total contribution by each class of planetesimal we should know the size distribution of the population. This is out of the scope of the present paper, but as a matter of speculation, if the distribution of mass is of the form $dn/dm \propto m^q$, for $q < -2$ small planetesimals dominate the distribution and we would not expect much water from planetesimals in terrestrial planets.

The behavior of the planetesimals for different disk profiles is shown in Figure 6. It

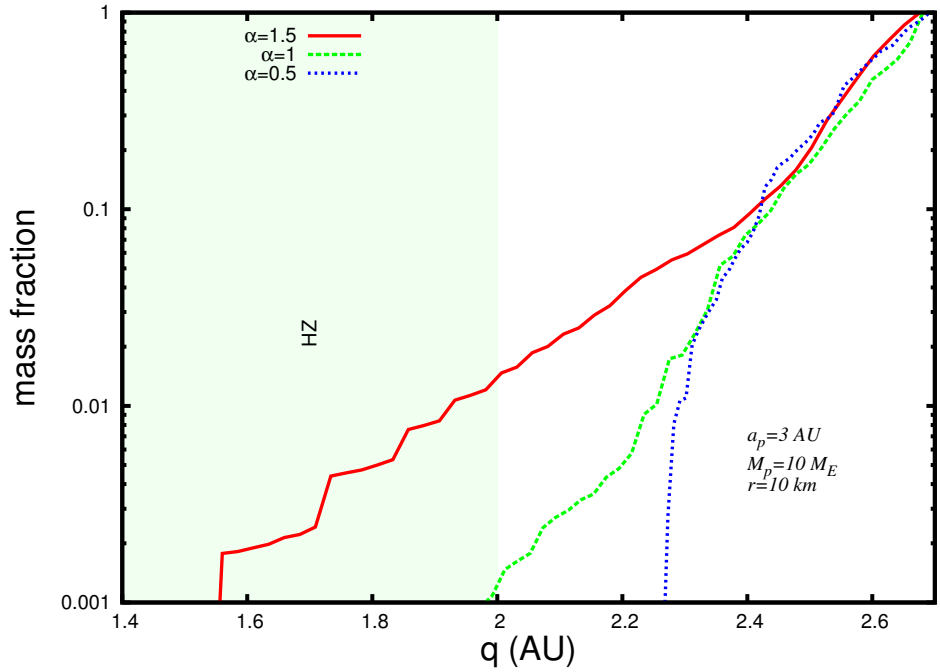

Figure 6: ***The fraction of water within the snow line delivered from beyond it for different profiles of the surface density of gas.***

The total mass of the disk is always 6 MMSN. Therefore, larger α means that more mass is beyond the snow line, and decay by gas drag is faster than for lower values of α. Sharp disk profiles favor the arrival of icy planetariums to the HZ.

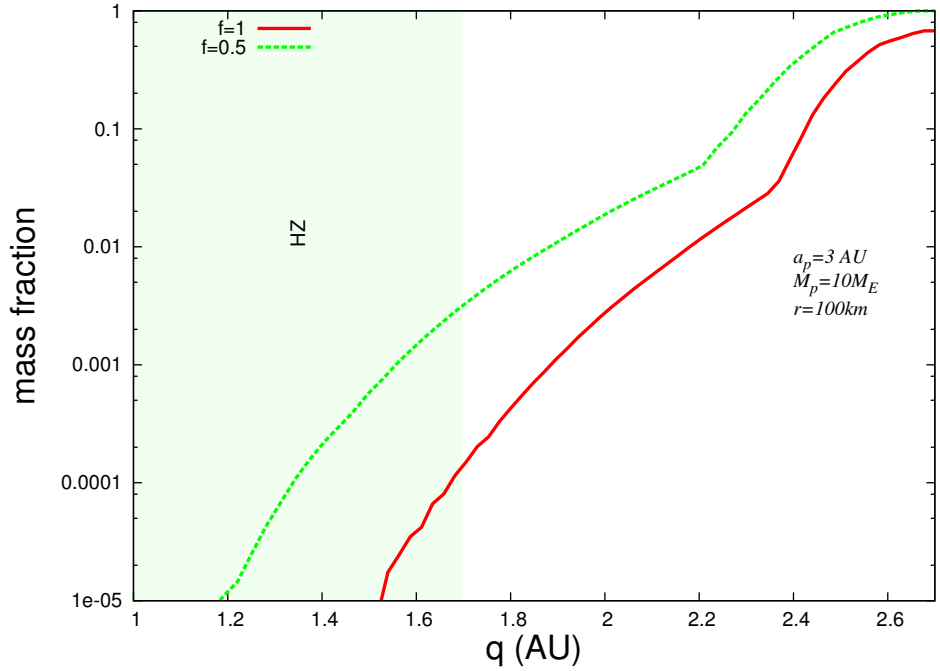

Figure 7: ***The fraction of water within the snow line for two different sublimation rates. For this case, values are normalized to the*** $f = 0.5$ ***case.***

If the rate of sublimation is reduced to a half, the mass of ice entering to the HZ increases by a factor of ~ 20.

4 Conclusions

We have presented here a first attempt to model the problem of the accretion by potentially habitable planets of primordial water carried by icy planetesimals born beyond the snow line.

Zain et al. (2018) claims that in planetary systems with small mass perturbers, the amount of water deposited by planetesimals coming from beyond the snow line is relevant. This is in contrast with our results, but not a surprise: They did not included in their model the sublimation of volatiles. Nevertheless their scenario have some differences with ours: In particular, they consider small stellar masses.

Our results show that the sublimation rate is a key parameter to address the amount of water entering to the HZ. Therefore, build up better models

of sublimation of ice would be mandatory. The possibility of a formation of a dust crust arouond icy objects on circular orbits is also a problem that need to be investigated.

Under the hypothesis of our model, icy planetesimals can only attain the HZ around solar type stars under certain conditions. They may be summarized as follows

1. The presence of a massive planet near the snow line seems to be an important factor. Without the planet-planetesimal dynamical interaction, outer planetesimals arrive to the snow line on circular orbits. Therefore, the sublimation rate is fast, acting on the whole orbit, and eroding planetesimal surface before reaching the HZ. Close encounters with a massive planet makes possible that planetesimals reach the HZ somewhat less eroded.

2. Only large planetesimals can reach the HZ.

3. Massive disks favor planetesimal ice to reach the HZ, because sublimation depends on the star radiation, but speed of migration by gas drag depends on the mass disk.

4. For a given disk mass, sharp density profiles are better to allow planetesimals to reach the HZ, because there is more mass of gas concentrated within the snow line.

Nevertheless, it seems that the contribution to the delivery of water by icy planetesimals during the early accretion phase would not be of fundamental relevance.

However, our calculations are limited in several aspects as to draw definitive answers. The presence of more than one massive planet, the interaction with existing terrestrial planets in the HZ and more importantly, some dynamical effects such a mean motion and/or secular resonances where the planetesimals can remain trapped by long times, or to be expelled to orbits of high eccentricity, could affect the amount of mass entering to the HZ in each particular case.

The snow line is not fixed at a given distance during all the accretionary phase. This is also an effect that can change the whole picture.

ACKNOWLEDGEMENTS we acknowledge the support by ITA (Institute of Applied Technology) of the Universidad Nacional de la Patagonia Austral.

References

Adachi I., Hayashi C., Nakazawa K., 1976, PThPh, 56, 1756

Banzatti A., Pinilla P., Ricci L., Pontoppidan K. M., Birnstiel T., Ciesla F., 2015, ApJ, 815, L15

Bell C. P. M., Naylor T., Mayne N. J., Jeffries R. D., Littlefair S. P., 2013, MNRAS, 434, 806

Blevins S. M., Pontoppidan K. M., Banzatti A., Zhang K., Najita J. R., Carr J. S., Salyk C., Blake G. A., 2016, ApJ, 818, 22

Brunini A., Benvenuto O. G., 2008, Icar, 194, 800

Chambers J., 2008, Icar, 198, 256

Chambers J. E., 2013, Icar, 224, 43

Chambers J. E., 2014, Icar, 233, 83

Chambers J. E., 2016, ApJ, 825, 63

Chambers J. E., Cassen P., 2002, M&PS, 37, 1523

Chyba C. F., 1987, Natur, 330, 632

Ciesla F. J., Mulders G. D., Pascucci I., Apai D., 2015, ApJ, 804, 9

Cieza L. A., et al., 2016, Natur, 535, 258

Delsemme A. H., 1984, OrLi, 14, 51

Delsemme A. H., 1992, AdSpR, 12, 5

Di Sisto R. P., Fernández J. A., Brunini A., 2010, IAUS, 263, 102

Dugaro A., de Elía G. C., Brunini A., Guilera O. M., 2016, A&A, 596, A54

Eker Z., Bilir S., Soydugan F., Gökçe E. Y., Soydugan E., Tüysüz M., Şenyüz T., Demircan O., 2014, PASA, 31, e024

Eker Z., et al., 2015, ASPC, 496, 295

Fernandez J. A., 1984, A&A, 135, 129

Fernández J. A., Gallardo T., Brunini A., 2002, Icar, 159, 358

Fernández J. A., 2005, ASSL, 328,

Fortier A., Benvenuto O. G., Brunini A., 2007, A&A, 473, 311

Haisch K. E., Jr., Lada E. A., Lada C. J., 2001, ApJ, 553, L153

Hernández J., Hartmann L., Calvet N., Jeffries R. D., Gutermuth R., Muzerolle J., Stauffer J., 2008, ApJ, 686, 1195-1208

Hayashi C., 1981, PThPS, 70, 35

Henon M., 1972, A&A, 19, 488

Ida S., Lin D. N. C., 2004a, ApJ, 604, 388

Ida S., Lin D. N. C., 2004b, ApJ, 616, 567

Ida S., Lin D. N. C., 2005, ApJ, 626, 1045

Ida S., Lin D. N. C., 2008a, ApJ, 673, 487-501

Ida S., Lin D. N. C., 2008b, ApJ, 685, 584-595

Ida S., Lin D. N. C., 2010, ApJ, 719, 810

Ida S., Lin D. N. C., Nagasawa M., 2013, ApJ, 775, 42

Ida S., Guillot T., 2016, A&A, 596, L3

Ip W.-H., Fernandez J. A., 1988, Icar, 74, 47

Izidoro A., Morbidelli A., Raymond S. N., 2014, ApJ, 794, 11

JeongAhn Y., Malhotra R., 2017, AJ, 153, 235

Johansen A., Mac Low M.-M., Lacerda P., Bizzarro M., 2015, SciA, 1, 1500109

Jorda L., Crovisier J., Green D. W. E., 1992, DPS, 24, 34.09-P

Kasting J. F., Whitmire D. P., Reynolds R. T., 1993, Icar, 101, 108

Kobayashi H., 2015, EP&S, 67, 60

Kopparapu R. K., 2013, ApJ, 767, L8

Kuehrt E., Keller H. U., 1994, Icar, 109, 121

Lammer H., et al., 2009, A&ARv, 17, 181

Lodders K., 2003, ApJ, 591, 1220

Lunine J. I., Chambers J., Morbidelli A., Leshin L. A., 2003, Icar, 165, 1

Matsumura S., Brasser R., Ida S., 2016, ApJ, 818, 15

Mamajek E. E., 2009, AIPC, 1158, 3

Miguel Y., Brunini A., 2008, MNRAS, 387, 463

Miguel Y., Brunini A., 2009, MNRAS, 392, 391

Miguel Y., Brunini A., 2010, MNRAS, 406, 1935

Miguel Y., Guilera O. M., Brunini A., 2011, MNRAS, 417, 314

Morbidelli A., Chambers J., Lunine J. I., Petit J. M., Robert F., Valsecchi G. B., Cyr K. E., 2000, M&PS, 35, 1309

Möhlmann D., 1995, P&SS, 43, 327

Mulders G. D., Ciesla F. J., Min M., Pascucci I., 2015, ApJ, 807, 9

Mizuno H., 1980, PThPh, 64, 544

O'Brien D. P., Morbidelli A., Levison H. F., 2006, Icar, 184, 39

O'Brien D. P., Walsh K. J., Morbidelli A., Raymond S. N., Mandell A. M., 2014, Icar, 239, 74

Oka A., Nakamoto T., Ida S., 2011, ApJ, 738, 141

Opik E. J., 1951, PRIA, 54, 165

Owen T. C., Bar-Nun A., 2001, OLEB, 31, 435

Rafikov R. R., 2004, AJ, 128, 1348

Raymond S. N., Quinn T., Lunine J. I., 2004, Icar, 168, 1

Raymond S. N., Scalo J., Meadows V. S., 2007, ApJ, 669, 606

Raymond S. N., Izidoro A., 2017, Icar, 297, 134

Ribas Á., Merín B., Bouy H., Maud L. T., 2014, A&A, 561, A54

Richert A. J. W., Getman K. V., Feigelson E. D., Kuhn M. A., Broos P. S., Povich M. S., Bate M. R., Garmire G. P., 2018, MNRAS,

Rickman H., Fernandez J. A., Gustafson B. A. S., 1990, A&A, 237, 524

Sato T., Okuzumi S., Ida S., 2016, A&A, 589, A15

Selsis F., 2007, leas.book, 199

Schäfer U., Yang C.-C., Johansen A., 2017, A&A, 597, A69

Simon J. B., Armitage P. J., Li R., Youdin A. N., 2016, ApJ, 822, 55

Simon J. B., Armitage P. J., Youdin A. N., Li R., 2017, ApJ, 847, L12

Tancredi G., Rickman H., Greenberg J. M., 1994, A&A, 286, 659

Tancredi G., Fernández J. A., Rickman H., Licandro J., 2006, Icar, 182, 527

Thommes E. W., Duncan M. J., Levison H. F., 2003, Icar, 161, 431

Walsh K. J., Morbidelli A., Raymond S. N., O'Brien D. P., Mandell A. M., 2011, Natur, 475, 206

Williams J. P., Cieza L. A., 2011, ARA&A, 49, 67

Zain, P. S., de Elía, G. C., Ronco, M. P., Guilera, O. M. A&A, 609, 76

Wetherill G. W., 1975, LPSC, 6, 1539